Available online at www.sciencedirect.com
ScienceDirect
Developmental Biology 303 (2007) 134–143
DEVELOPMENTAL BIOLOGY
www.elsevier.com/locate/ydbio

Role of the hindbrain in patterning the otic vesicle: A study of the zebrafish *vhnf1* mutant

Virginie Lecaudey [a,1], Encarna Ulloa [b], Isabelle Anselme [a], Aline Stedman [a], Sylvie Schneider-Maunoury [a], Cristina Pujades [b,*]

[a] *Unité de Biologie du Développement, CNRS UMR 7622, Université Pierre et Marie Curie, Paris, France*
[b] *Departament de Ciències Experimentals i de la Salut, Universitat Pompeu Fabra, Parc de Recerca Biomèdica, C/ Dr. Aiguader 80, 08003, Barcelona, Spain*

Received for publication 7 June 2006; revised 27 October 2006; accepted 27 October 2006
Available online 1 November 2006

Abstract

The vertebrate inner ear develops from an ectodermal placode adjacent to rhombomeres 4 to 6 of the segmented hindbrain. The placode then transforms into a vesicle and becomes regionalised along its anteroposterior, dorsoventral and mediolateral axes. To investigate the role of hindbrain signals in instructing otic vesicle regionalisation, we analysed ear development in zebrafish mutants for *vhnf1*, a gene expressed in the caudal hindbrain during otic induction and regionalisation. We show that, in *vhnf1* homozygous embryos, the patterning of the otic vesicle is affected along both the anteroposterior and dorsoventral axes. First, anterior gene expression domains are either expanded along the whole anteroposterior axis of the vesicle or duplicated in the posterior region. Second, the dorsal domain is severely reduced, and cell groups normally located ventrally are shifted dorsally, sometimes forming a single dorsal patch along the whole AP extent of the otic vesicle. Third, and probably as a consequence, the size and organization of the sensory and neurogenic epithelia are disturbed. These results demonstrate that, in zebrafish, signals from the hindbrain control the patterning of the otic vesicle, not only along the anteroposterior axis, but also, as in amniotes, along the dorsoventral axis. They suggest that, despite the evolution of inner ear structure and function, some of the mechanisms underlying the regionalisation of the otic vesicle in fish and amniotes have been conserved.

Keywords: *vhnf1*; Otic vesicle; Inner ear; Hair cells; Zebrafish; Hindbrain

Introduction

The inner ear of vertebrates is a complex sensory organ responsible for hearing, balance and sensing acceleration. It derives from the otic placode, an ectodermal thickening that forms lateral to the hindbrain. In zebrafish, the otic placode can first be recognised morphologically at about the 9–10 somites stage (13.5–14 hours post-fertilization, hpf), as an oval grouping of cells within the ectoderm. Then, by 18 hpf, the placode cavitates to form a hollow vesicle that develops into the inner ear (Haddon and Lewis, 1996).

The two sensory cell types of the inner ear – the hair cells of the sensory patches and the sensory neurons of the statoacoustic ganglion (SAG) – originate from specific regions of the otic vesicle. The sensory neurons derive from neuroblasts that originate within the anteroventral region of the otic epithelium, and delaminate to form the SAG close beneath (Andermann et al., 2002; Haddon and Lewis, 1996). The sensory patches are thickened regions of the otic epithelium, consisting of arrays of hair cells and supporting cells generated by lateral inhibition mediated by Notch signalling (Haddon et al., 1998a). The utricular and saccular maculae are the first sensory patches to develop, in the anteroventral and posteromedial regions of the otic vesicle, respectively. Each is overlain by an otolith (Haddon and Lewis, 1996; Whitfield et al., 2002). Beneath each otolith and apparently attached to their tips are the first sensory hair cells, called tether cells. The three cristae, the sensory patches for each of the three semicircular canals, differentiate later, around 72 hpf, within the lateral wall of the vesicle.

Development of the inner ear requires interaction with the adjacent hindbrain tissue. Many studies have shown that

* Corresponding author. Fax: +34 935422802.
E-mail address: cristina.pujades@upf.edu (C. Pujades).
[1] Present address: EMBL Heidelberg, Meyerhofstrasse 1, D-69117 Heidelberg, Germany.

0012-1606/$ - see front matter © 2006 Elsevier Inc. All rights reserved.
doi:10.1016/j.ydbio.2006.10.041

hindbrain signals induce the otic placode in the adjacent surface ectoderm, within a domain that extends from the posterior end of rhombomere 4 down to rhombomere 6 (Whitfield et al., 2002; Torres and Giraldez, 1998). In addition to otic placode induction, the hindbrain was proposed to provide signals that specify positional information within the otic vesicle (Brigande et al., 2000; Fekete, 1999). However, the axes and structures specified seem to be different depending on the species. Several lines of evidence, ranging from early transplantation experiments in chick (Giraldez, 1998) to gene inactivation studies in mice (Chang et al., 2004; Riccomagno et al., 2002, 2005; Bok et al., 2005) indicate that in amniotes, hindbrain signals are required to specify structures along the dorsoventral (DV) axis of the inner ear. Shh signalling from the notochord and floor plate is required for the formation of the cochlea, a ventral otocyst-derived structure, while Wnt signals from the dorsal neural tube are essential for the morphogenesis of the vestibular apparatus, a dorsal otocyst-derived structure (Riccomagno et al., 2002, 2005). The *MafB* gene, expressed in rhombomeres 5 and 6, is also involved in DV patterning of the ear. In the *kreisler* mouse mutant, in which expression of the *MafB* gene in the caudal hindbrain is abolished, the cochlea is expanded and dorsal structures such as the endolymphatic duct are absent (Choo et al., 2006). In fish, however, signals from the neural tube have been shown to be involved in anteroposterior (AP) patterning of the otic vesicle. Zebrafish embryos in which the *valentino* gene (*val*, the zebrafish orthologue of *MafB/kreisler*) is inactivated show defects in AP patterning of the otic vesicle (Kwak et al., 2002). These defects are due, at least in part, to an expansion of Fgf3 signalling within the hindbrain. These data suggests that, in addition to being necessary for its induction (Leger and Brand, 2002), Fgfs from the hindbrain are also involved in the AP patterning of the zebrafish otic placode (Kwak et al., 2002; Leger and Brand, 2002). Surprisingly, in zebrafish as well, Hedgehog (Hh) signalling is involved in AP patterning of the otic vesicle, rather than in DV or mediolateral (ML) patterning as predicted by the mouse studies (Hammond et al., 2003).

The recent isolation of mutant alleles of the *vhnf1* gene in the zebrafish provides an additional model in which to study the role of hindbrain signals in otic vesicle development (Sun and Hopkins, 2001). *vhnf1* codes for a homeodomain transcription factor and is involved in caudal hindbrain patterning in zebrafish embryos. This gene is expressed from the end of gastrulation onwards, in a caudal domain of the neural tube with an anterior limit that coincides with the prospective r4/r5 boundary (Lecaudey et al., 2004; Sun and Hopkins, 2001; Wiellette and Sive, 2003). The analysis of *vhnf1* mutant embryos has demonstrated that this transcription factor acts in synergy with Fgf signals from prospective r4, to activate the expression of *val* in r5 and r6, and of *krx20* in r5 (Hernandez et al., 2004; Maves et al., 2002; Sun and Hopkins, 2001; Walshe et al., 2002; Wiellette and Sive, 2003). In addition, *vhnf1* represses the expression of *hoxb1a*, the functional homologue of mouse *Hoxb1*, independently of Fgf signals, thereby limiting its expression to prospective r4 (Hernandez et al., 2004; Wiellette and Sive, 2003). Although *vhnf1* is not expressed in the inner ear, *vhnf1* mutants display otic vesicles that are small and malformed.

To further examine the importance of hindbrain signals in instructing otic vesicle development, we have investigated otic vesicle patterning in *vhnf1*^{hi2169} mutants (Sun and Hopkins, 2001). Our results support a model in which *vhnf1* expression within the posterior neural tube (up to r5) promotes posterior and dorsal fates in the otic vesicle, at the expense of anterior and ventral fates. Thereby, in zebrafish, hindbrain signals are involved in both AP and DV patterning of the inner ear.

Materials and methods

Zebrafish lines, maintenance and genotyping

Zebrafish (*Danio rerio*) were raised and staged as previously described (Kimmel et al., 1995). The *vhnf1*^{hi2169} mutant line has been described previously (Sun and Hopkins, 2001). Embryos were genotyped either by PCR on tail clips (Sun and Hopkins, 2001) or by *in situ* hybridisation, using *krx20* or *frb35* as r5 markers. Sun and Hopkins (2001) have shown that r5 is strongly reduced in *vhnf1*^{hi2169} homozygous embryos. In order to validate r5 size as a readout of the genotype of *vhnf1* embryos, we genotyped by PCR 14 and 24 hpf embryos from crosses of *vhnf1* heterozygous parents and measured the surface area of r3 and of r5 on dorsal views of these embryos. We then calculated the ratio of r5 over r3 surface area (r3 is not affected in *vhnf1* mutant embryos). At 14 hpf, the surface area ratio was: for wt embryos, 1.13 ± 0.16 ($n=8$), for heterozygous embryos, 1.13 ± 0.12 ($n=16$), and for homozygous embryos, 0.30 ± 0.09 ($n=24$). At 24 hpf, the ratio was, for wt embryos, 1.56 ± 0.13 ($n=2$), for heterozygous embryos, 1.31 ± 0.15 ($n=3$), and for homozygous embryos, 0.29 ± 0.08 ($n=8$). Therefore, all *vhnf1* homozygous embryos present a reduction of the r5 surface area of about 4 to 5 fold as compared to control (wt and heterozygous) embryos.

Quantitative analysis of the phenotype

For each experiment the ratio of affected embryos was expressed as *x/y*, where *x* is the number of affected embryos and *y* is the total number of homozygous mutant embryos. Mutant phenotypes were sometimes unilateral. When ratios were expressed in number of ears instead of number of embryos, this is clearly stated in the text.

Viewing live embryos with Differential Interference Contrast (DIC)

For direct observation, embryos were anaesthetised in tricaine (10 mg/ml) and mounted on methyl cellulose in embryo medium (Westerfield, 1995). Analysis was carried out using a Nikon Eclipse E800 microscope.

Whole mount in situ hybridisation and immunostaining

Whole-mount *in situ* hybridisation was carried out as described previously (Hauptmann and Gerster, 1994). The following probes were used: *dlx3b* (Akimenko et al., 1994), *deltaA* (Haddon et al., 1998b), *deltaD* (Haddon et al., 1998b), *eya1* (Sahly et al., 1999), *fgf8* (Reifers et al., 1998), *follistatin* (Bauer and Goetz, 1998), *frb35* (Sun et al., 2002), *krx20* (Oxtoby and Jowett, 1993), *msxC* (Ekker et al., 1997), *ngn1* and *neuroD* (Blader et al., 1997), *nkx5.1* (Adamska et al., 2000), *pax2a* (Krauss et al., 1991), *pax5* (Pfeffer et al., 1998), *serrateB* (Haddon et al., 1998a), *wnt1* (Molven et al., 1991), *wnt3a* (Krauss et al., 1992) and *zath1* (Itoh and Chitnis, 2001). Immunostainings were performed as described previously (Westerfield, 1995) using the monoclonal antibodies against acetylated tubulin (Sigma T-6793, 1:500) and Islet1 (DSHB 39.4D5, 1:30). Images were taken under a Nikon Eclipse E800 microscope, except for acetylated tubulin immunofluorescence images, which were taken under a Leica DM IRBE confocal microscope.

Phalloidin staining

Embryos were fixed in 4% PFA in PBS at 4 °C and rinsed in PBS containing 2% Triton X100 to permeabilise the tissue. Specimens were left to soak for 1 or

2 days until the calcareous otoliths had disappeared. Embryos were stained with FITC-labelled phalloidin (Sigma P5282) according to Haddon and Lewis (1996). Images were taken on a Leica DM IRBE scanning confocal microscope.

Results

The morphology of the inner ear is abnormal in vhnf1 mutants

During zebrafish development, the otic placode first becomes visible around 13.5–14 hpf as a thickening of the ectoderm lateral to r4–r6. The placode then cavitates to generate the otic vesicle, which contains two otoliths in stereotyped locations at opposite ends of the vesicle (Haddon and Lewis, 1996). It has previously been reported that the otic vesicles of *vhnf1* homozygous mutant embryos at 22 hpf are smaller than those of wild type embryos (Sun and Hopkins, 2001). However, the morphological and molecular aspects of this defect have not been investigated so far. We analysed in detail the morphogenetic defects of the inner ear in *vhnf1* mutants at later stages of embryonic development. In mutant embryos at 28 hpf, the otic vesicle was rounded in shape when compared with the ovoid shape of the wild type ear (Figs. 1a–c). This change of morphology correlated with a reduction in the AP length of the vesicle (101±6 μm in homozygous embryos (n=15) versus 125±8 μm in control embryos (n=9), p<0.005), combined with a slight expansion of its DV length (75±8 μm in homozygous embryos (n=15) versus 64±10 μm in control embryos (n=9) p<0.01). In all the mutants (n=12) two otoliths formed but their size and distribution varied considerably, and usually the caudal otolith had an irregular shape (8/12). In wild type embryos, the three protrusions of the walls of the otic vesicle that will form the semi-circular canals were detected at 52 hpf (Fig. 1d), and by 72 hpf they were fused in the middle (Fig. 1g) (Haddon and Lewis, 1996). In *vhnf1* mutant embryos at 52 hpf, canal protrusions also formed, but with abnormal number and shape (Figs. 1e, f). Morphogenetic defects of the semicircular canals were observed in all homozygous mutant embryos at 72 hpf (Figs. 1h, 4i) (6/6).

Previous studies have implicated hindbrain signals in otic placode induction (Whitfield et al., 2002). Hence, the reduction in size of the otic vesicle in *vhnf1* mutants could be due to impaired placode induction. In order to investigate this possibility, we performed *in situ* hybridisation experiments with the placodal marker *eya1* at 14 hpf, a stage when the otic placode is well individualised. As shown in Figs. 1j, k, the size of the otic placodes was not significantly different between *vhnf1* homozygous mutant (n=4) and control embryos (n=4). Accordingly, similar results were obtained with *pax2a*, an early marker of the presumptive otic placode (Hans et al., 2004) (Figs. 1l, m). The size of the otic *pax2a*-positive domain was similar in wild type (98±13 μm, n=5) and homozygous mutant (96±9 μm, n=8) embryos. Although *pax2a* has not been formally demonstrated to be a specific otic placode marker at this stage, our results strongly suggest that the reduction in size of the otic vesicles in *vhnf1* mutants is not due to an early defect in otic induction.

Anteroposterior (AP) patterning of the otic vesicle is altered in vhnf1 mutants

We then investigated whether the abnormal morphology of the otocysts of *vhnf1* mutant embryos may result from defects in

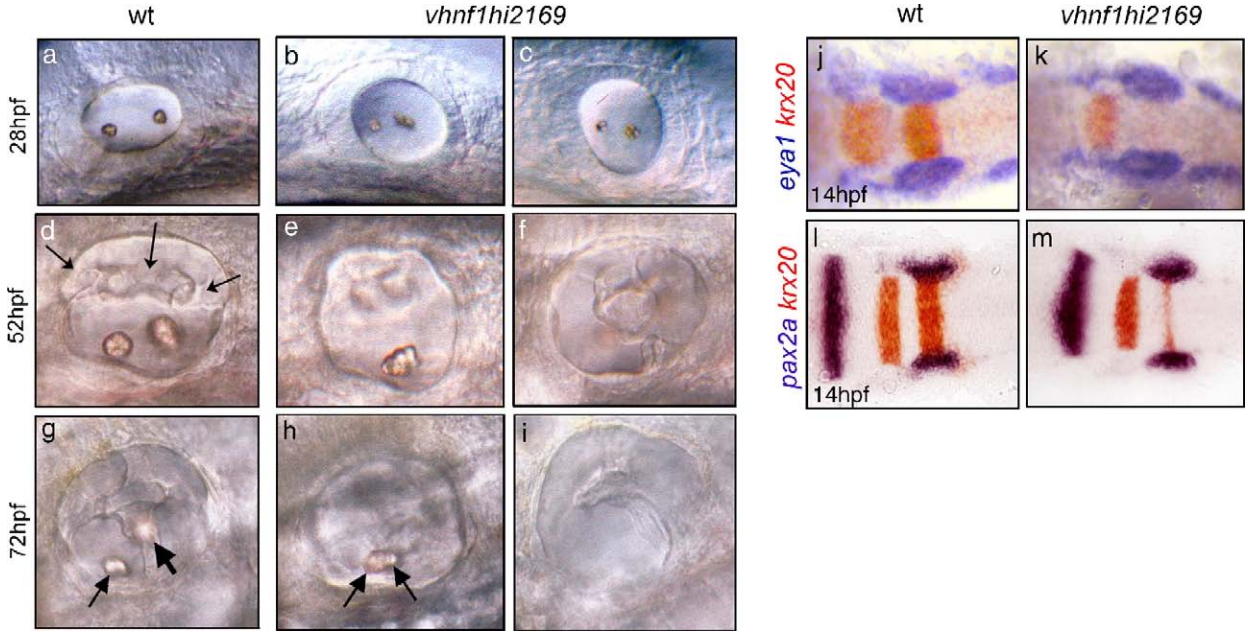

Fig. 1. Morphology of the inner ear in *vhnf1*^{hi2169} mutants. (a–i) DIC images of developing inner ears of wild type (a, d, g) and *vhnf1*^{hi2169} (b, c, e, f, h, i) homozygous live embryos at different developmental stages (as indicated). Lateral views (anterior to the left, dorsal to the top). (j–m) Whole mount double *in situ* hybridisation in 14 hpf wild type (j, l) and *vhnf1*^{hi2169} (k, m) embryos with probes for *eya1* (j, k) or *pax2a* (l, m) in blue, and *krx20* in red. *krx20* staining was used to position r5 and to measure the extent of r5 loss. Dorsal views (anterior to the left). Arrows in (d) indicate the epithelial protusions that will form the semicircular canals. Arrows in (g, h) indicate the otoliths.

otic patterning. Since the otic vesicles of *vhnf1* mutant embryos appeared shorter along the AP axis, we first analysed genes expressed in restricted AP domains of the otic vesicle. *nkx5.1* is the earliest known marker of an asymmetry along the AP axis of the otic placode (Adamska et al., 2000; Hammond et al., 2002; Pfeffer et al., 1998). Already at 14 hpf, *nkx5.1* expression was restricted to the anterior aspect of the otic placode (Fig. 2a). In *vhnf1* mutant embryos, the *nkx5.1* expression domain was dramatically expanded as early as the 14 hpf stage (Fig. 2b). This expansion persisted in the otic vesicle until at least 30 hpf (Figs. 2c–f). The phenotypes ranged from the duplication of the anterior *nkx5.1* expression domain in the posterior part of the vesicle (9/42), to an expansion of this expression domain to the whole AP extent of the vesicle (33/42) (Figs. 2a–f). Two other genes, *fgf8* and *pax5,* are expressed in the anterior region of the otic vesicle at 24 hpf (Figs. 2g, j) (Hammond et al., 2003). In *vhnf1* mutants, the expression domains of both genes were always affected (Figs. 2h, i, k, l). Some of the mutant embryos displayed a duplication of the *fgf8*- (7/13) or *pax5*-positive domain (12/24) in the posterior part of the otic vesicle (Figs. 2h, k). Interestingly, the expression domains of *fgf8* and *pax5* in *vhnf1* mutant embryos had also significantly extended dorsally compared to the wild type situation. The most affected embryos even presented a single dorsal expression domain (Figs. 2i, l; 6/13 for *fgf8* and 12/24 for *pax5*) (see below for further details).

In order to determine whether the anterior region of the otic vesicle in *vhnf1* mutants was expanded at the expense of posterior territories, we analysed the expression of the posterior marker *follistatin*. In wild type embryos, *follistatin* was expressed in the most posterior part of the otic vesicle at 26 hpf (Fig. 2m) (Hammond et al., 2003). In some *vhnf1* embryos, *follistatin* expression was reduced or absent (Fig. 2n) (4/14). Interestingly, in many mutant embryos, the *follistatin*-expression domain was still present but located at a more dorsal position within the otic vesicle (Fig. 2o) (9/14).

Altogether, *vhnf1* mutants show a strong anteriorisation of the entire otic vesicle by the time AP asymmetry first arises in wild type embryos. This is consistent with the hypothesis that factors locally expressed in the hindbrain regulate anteroposterior fates in the medial wall of the otic vesicle, and that such factors are misregulated in *vhnf1* mutants.

Otic patterning along the dorsoventral (DV) axis is affected in vhnf1 mutant

During the analysis of otic AP patterning, we observed that the expression domains of *fgf8* and *pax5* were also modified along the DV axis. The expression of these genes is normally restricted not only to the anterior but also to the ventral aspect of the otic vesicle (Figs. 2g, j). In *vhnf1* mutants, the expression of *fgf8* and *pax5* was always shifted dorsally (Figs. 2h, i, k, l). In the most affected embryos, a unique dorsal expression domain was observed (Figs. 2i, l), suggesting that the duplicated gene expression domains had fused dorsally.

In order to confirm these data, we analysed the expression of the proneural gene *zath1*. *zath1* is expressed at 27 hpf in the two anteroventral and posteroventral domains of the otic vesicle. These domains are adjacent to r4 and r6 and prefigure the utricular and saccular maculae, respectively (Fig. 3a) (Whitfield et al., 2002). In *vhnf1* mutants, cells expressing *zath1* were found in the dorsal region of the otic vesicle (8/8) (Figs. 3b, c). Again, in several cases the *zath1* expression domains were so dorsally shifted that they fused to form a single domain spanning the whole dorsal wall of the otic vesicle (5/8) (Fig. 3c).

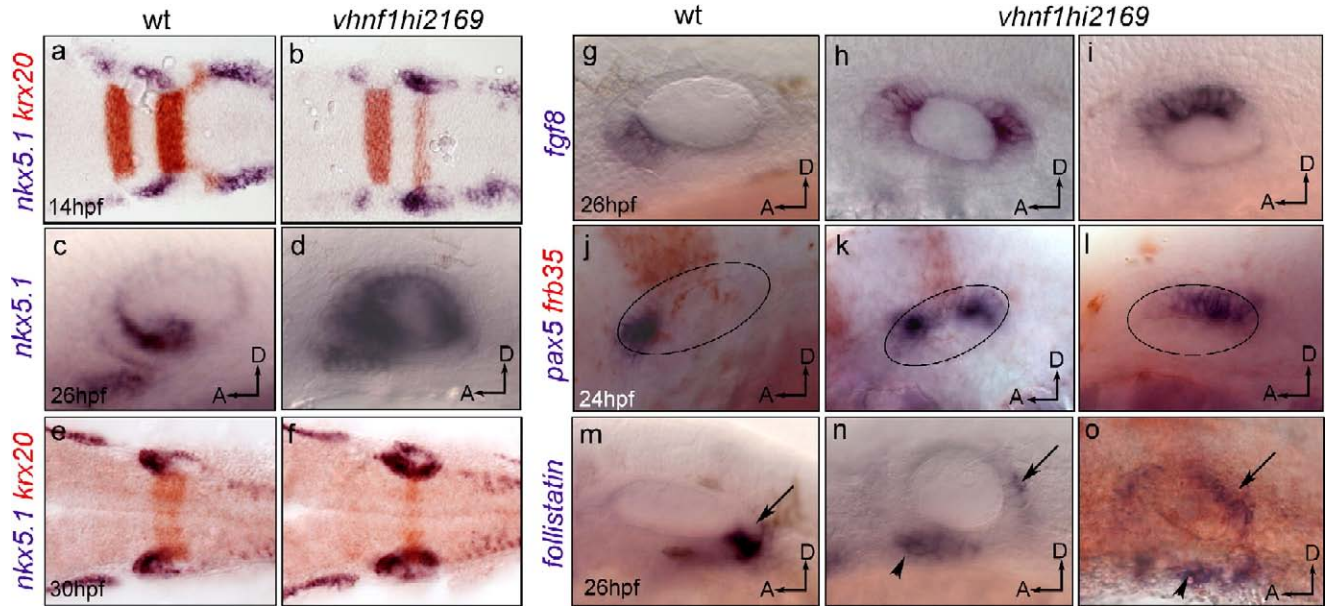

Fig. 2. Anteroposterior patterning of the otic vesicle in *vhnf1* mutant embryos. Whole mount single (c, d, g–i, m, n) or double (a, b, e, f, j–l, o) *in situ* hybridisations in wild type (a, c, e, g, j, m) or *vhnf1* mutant (b, d, f, h, i, k, l, n, o) embryos with probes for *nkx5.1* (a–f), *fgf8* (g–i), *pax5* (j–l) and *follistatin* (m–o) in blue, at different developmental stages (as indicated). For double *in situ* hybridisation either *krx20* (a, b, e, f) or *frb35* (j–l, o) in red were used to position r5. (a, b, e) and (f) are dorsal views. (c, d) and (g–o) are lateral views. Anterior is to the left in all pictures. Arrows in (m–o) indicate the staining in the otic epithelium and head arrows the staining outside the otic vesicle.

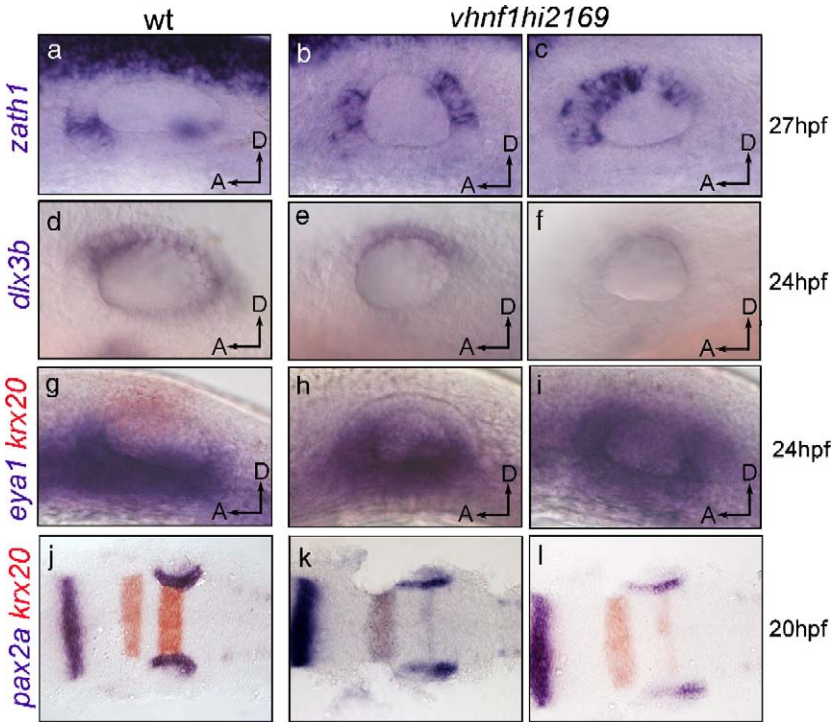

Fig. 3. Patterning along the dorsoventral and mediolateral axes in *vhnf1* otic vesicles. (a–i) Whole mount *in situ* hybridisation with probes for *zath1* (a–c), *dlx3b* (d–f), *eya1* in blue and *krx20* in red (g–i) in control (a, d, g) and *vhnf1* mutant (b, c, e, f, h, i) embryos. Developmental stages are indicated. Lateral views, anterior to the left. (j–l) Double *in situ* hybridisation at 20 hpf with probes for *pax2a* in blue and *krx20* in red. Dorsal views, anterior to the left.

We further investigated the DV patterning defects by analysing the expression of the *dlx3b* gene. *dlx3b* is normally expressed in the dorsal epithelium at 24 hpf (Fig. 3d) (Hammond et al., 2003). However, in *vhnf1* homozygous mutant embryos, the expression domain of *dlx3b* was severely reduced (7/8) (Figs. 3e, f). We also analysed the expression of *eya1*, which marks the ventral domain of the otic vesicle in wild type embryos (Fig. 3g). In *vhnf1* mutants, *eya1* expression was moderately expanded (Figs. 3h, i): in homozygous embryos 65%±2% of the otic vesicle perimeter was positive for *eya1* ($n=7$), whereas in control embryos *eya1*-positive domain covered only 55%±3% of the otic perimeter ($n=7$).

Finally, we investigated otic patterning along the mediolateral (ML) axis. We used *pax2a* at 18 hpf and *nkx5.1* at 30 hpf as medial otic markers (Fig. 3j, Fig. 2e). In *vhnf1* mutants as in wild type embryos, *pax2a* and *nkx5.1* expression was restricted to the medial wall of the otic vesicle (Figs. 3j–l and 2e–f), suggesting that ML patterning is not affected in *vhnf1* mutants.

These results show that otic patterning along DV axis is significantly perturbed in *vhnf1* mutants. The duplicated antero- and postero-ventral domains of the vesicle are shifted dorsally, leading in the most affected embryos to a unique fused domain in the dorsal part of the mutant otic vesicle. Mediolateral patterning appears unaffected.

Dorsal signals from the neural tube are affected in vhnf1 embryos

In order to investigate which neural tube signals, downstream of *vhnf1*, could be involved in the DV patterning defects of the inner ear described above, we checked for the expression of *wnt1* and *wnt3a*, two genes normally expressed in the dorsal hindbrain (Molven et al., 1991; Krauss et al., 1992; Riley et al., 2004). *wnt1* was expressed all along the most dorsal part of the hindbrain, very strongly in r5 and faintly in r6 (Fig. 4a) in control embryos. The r5-high level expression domain was absent in all *vhnf1* homozygous embryos, consistent with the loss of r5 (3/3) (Fig. 4b). *wnt3a* was expressed strongly in the

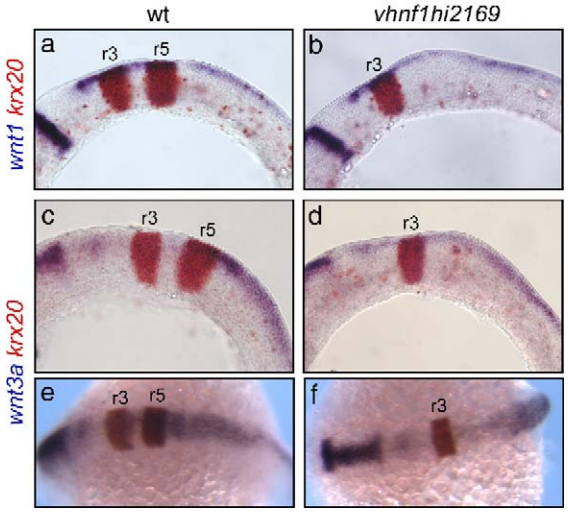

Fig. 4. Neural tube signals in *vhnf1* embryos. Whole mount double *in situ* hybridisations in wild type (a, c, e) or *vhnf1* mutant (b, d, f) embryos at 16 hpf with probes for *wnt1* (a–b), *wnt3a* (c–f) in blue, and *krx20* in red. (a–d) are lateral views, (e, f) are dorsal views. Anterior is to the left.

hindbrain caudal to r5 in control embryos (Figs. 4c, e). *vhnf1* mutant embryos displayed a clear reduction of *wnt3a*-expression in the caudal hindbrain (7/7) (Figs. 4d, f). These results show that Wnt signals from the dorsal hindbrain are reduced in *vhnf1* mutant embryos.

Sensory patches are disrupted in vhnf1 mutants

The sensory hair cells of the inner ear originate from the ventral part of the otic vesicle and begin to differentiate very early. The first hair cells arise in two small patches, at the anterior and posterior ends of the otocyst, that form the utricular and saccular maculae (Haddon and Lewis, 1996; Riley et al., 1997). By 72 hpf, three additional sensory patches, the cristae, become visible. This precise spatial arrangement of sensory elements is probably set up by early patterning processes in the otic vesicle. To investigate this possibility, we tested whether the patterning defects observed in the otic vesicle of *vhnf1* mutant embryos resulted in a later disorganization of the sensory elements.

Differentiated hair cells are identified by their stereociliary bundles, which are first seen at about 24 hpf. By 85 hpf, the differentiated hair cells within the sensory patches can be visualised by staining with FITC-phalloidin, which binds the bundles of hair cells (Haddon and Lewis, 1996). The ears of wild type embryos displayed a stereotyped pattern of sensory patches, with the anterior macula (am) sitting on the anteroventral floor, the posterior macula (pm) on the posteromedial wall, and the three cristae (ac, lc, pc) lying at distinct AP positions of the lateral wall (Fig. 5a). In *vhnf1* homozygous mutant embryos, the number, distribution and size of the sensory patches were abnormal, and exhibited erratic patterns of organization (8/8) (Figs. 5b, c). This organization of the sensory patches was highly variable among individuals.

The presence of hair cells in ectopic positions in *vhnf1* mutant inner ears was also illustrated by immunostaining for acetylated tubulin at 30 hpf. At this stage, tether cells, the first hair cells to differentiate, are characterized by the presence of long kinocilia at their apical side, stained by acetylated tubulin. These cilia are much longer than the primary cilia present on the

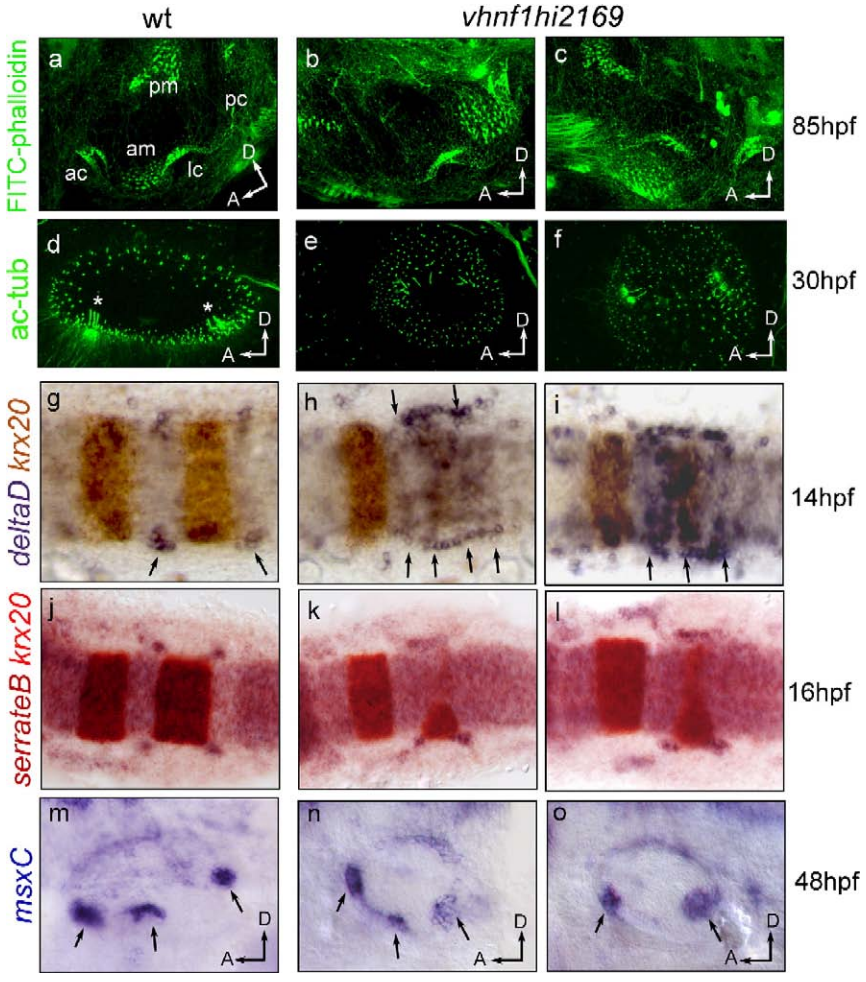

Fig. 5. Formation of sensory patches in *vhnf1* mutants. Control (a) and *vhnf1* mutant (b, c) embryos stained for FITC-phalloidin in order to label differentiated hair cells at 85 hpf. Lateral views. (d–f) Immunostainings with anti-acetylated tubulin at 30 hpf, in control (d) and mutant (e, f) embryos. Lateral views. (g–l) Double *in situ* hybridisations on control (g, j) or *vhnf1* mutant (h, i, k, l) embryos with probes for *deltaD* (g–i) and *serrateB* (j–l) in blue and for *krx20* (g–l) in red. Dorsal views. (m–o) *In situ* hybridisation with a probe for *msxC* on control (m) and mutant (n, o) embryos at 48 hpf. Lateral views. Asterisks in (d) mark the two patches of tether cells. Arrows in (g–i) point to cells of the otic sensory patches. Arrows in (m–o) point to the cristae. Anterior is always to the left.

luminal side of other cells in the vesicle. In control embryos, tether cells form two small groups at the most anterior and posterior aspect of the otic vesicle (Fig. 5d) (Riley et al., 1997). In *vhnf1* mutants, the two patches of tether cells were either closer to each other, with one of them located at a more dorsal position (3/7) or fused in the middle of the otic vesicle (3/7) (Figs. 5e, f).

In order to better understand the disruption of the hair cell organization, we analysed earlier stages of sensory organ development. Several genes, in addition to *zath1*, mark the positions of sensory patches in the otic placode well before the differentiation of hair cells. Neurogenic genes of the Delta/Serrate family of Notch ligands (*deltaA, B, D*, and *serrateB*) are expressed in very similar patterns as early as the 10 somite stage (14 hpf) in two small groups of cells, that prefigure the future utricular and saccular maculae (Figs. 5g, j, and data not shown) (Haddon et al., 1998a; Whitfield et al., 2002). We first analysed the expression of *deltaD* in *vhnf1* mutant embryos at 14 hpf. In these embryos, *deltaD*-expressing cells were found all along the length of the AP axis of the otic placode (8/8) (arrows in Figs. 5h, i). Similar results were obtained with *serrateB* (6/6) (Figs. 5k, l) and *deltaA* (data not shown). These results are consistent with the expansion of the *zath1*-positive domains at later stages (Figs. 3a–c) and show that positioning of sensory patches is incorrect in *vhnf1* mutant embryos.

The organization of the later formed sensory patches, the cristae, was studied by analysing the expression of *msxC* (Ekker et al., 1997; Mowbray et al., 2001). In control embryos at 48 hpf, *msxC* was expressed in three discrete ventral domains corresponding to the anterior, lateral and posterior cristae (Fig. 5m). In the majority of *vhnf1* mutant ears, only two *msxC* expression domains were observed (10/12 ears) (Fig. 5o), although in few cases one patch with the normal size (anterior), a very small middle patch, and a big posterior patch were found (Fig. 5n). One of the *msxC*-positive patches was bigger, suggesting that it corresponds to the fusion of two cristae. Due to the lack of specific markers for individual cristae, we were unable to assign an identity to the mutant cristae.

In summary, in *vhnf1* mutants, sensory patches are specified ectopically along the entire AP axis of the otic placode. Accordingly, at the otic vesicle stage hair cells emerge in ectopic locations along the AP and DV axes. We propose that the mechanisms that normally restrict the spatial specification of the sensory patches are disrupted in these mutants.

Neurogenesis and formation of the stato-acoustic ganglion (SAG)

The primary sensory neurons derive from the neuroblasts that originate within the anteroventral region of the otic vesicle. By 22 hpf, neuroblasts delaminate from the otic epithelium to form the SAG (Andermann et al., 2002; Haddon and Lewis, 1996). Two proneural genes coding for bHLH transcription factors, *ngn1* and *neuroD,* are expressed in these neuroblasts. *ngn1* expression is transient and preceeds the expression of *neuroD.* As the otic placode develops into a vesicle, the neuroblasts begin to transiently express *ngn1* before delaminating. *neuroD* is expressed in neuroblasts just before their delamination but persists in these cells as they coalesce into the ganglion (Andermann et al., 2002).

In order to determine whether *vhnf1* is required for sensory neuron formation, we analysed the expression of *ngn1* and *neuroD* from 24 to 48 hpf. In control embryos at 24 hpf, cells expressing *neuroD* and *ngn1* were observed in the most anterior region of the otic placode – the neurogenic region – (Fig. 6a). In *vhnf1* mutant embryos, *neuroD*- and *ngn1*-positive cells were detected in a broader domain of the otic vesicle (9/12 ears) (Fig. 6b). Duplications of the neurogenic region were never observed. After delamination, neuroblasts start to express the neuronal marker Isl1. To determine whether this expanded neurogenic domain gives rise to more sensory neurons and results in a bigger SAG, we carried out immunostainings for Isl1, which labels the neurons of this ganglion. At 30 hpf, the size of the SAG was not significantly different in wild type and *vhnf1* mutant embryos (Figs. 6c, d) and no ectopic posterior ganglion was found (Fig. 6d).

In the otic epithelium, the peak period of delamination is from 22 hpf to 28 hpf, and by 42 hpf there is no longer any sign of delamination (Haddon and Lewis, 1996). Accordingly, in wild type embryos at 48 hpf, epithelial cells of the otic vesicle did not express *ngn1* (Fig. 6e). In contrast, in homozygous mutant embryos, *ngn1*- and *neuroD*-expressing cells were still present within the otic epithelium at this stage (6/6 ears) (Figs. 6f, g, and data not shown).

In summary, these data show that the expansion of the anterior otic region correlates with an expanded neurogenic

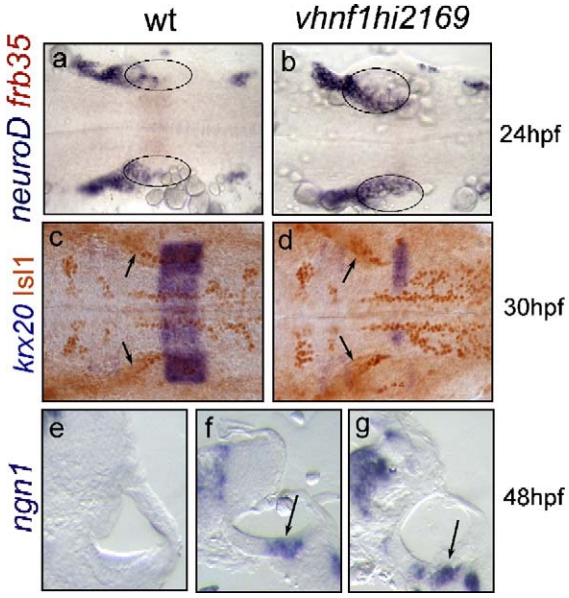

Fig. 6. Otic neuroblast generation in *vhnf1* mutants. Wild type (a, c, e) and *vhnf1* mutant (b, d, f, g) embryos were analysed for neuroblast generation. (a, b) Whole mount *in situ* hybridisation with probes for *neuroD* in blue, and *frb35* in red. (c, d) Combined immunohistochemistry with an Isl1 antibody (in brown) and *in situ* hybridisation with a probe for *krx20* (in blue). Roughly, the SAG cells lie at and posterior to the anterior end of the otocyst (arrows in c and d). (e–g) *In situ* hybridisation with a probe for *ngn1*. (a–d) are dorsal views with anterior to the left. (e–g) are transverse sections. Arrows in (f) and (g) point to cells expressing *ngn1* within the otic epithelium.

region. In addition, genes normally expressed before delamination remain expressed longer in the mutant. However, this does not lead to an increase in the size of the SAG, suggesting that the final specification of the sensory neurons and/or the size of the SAG are controlled by mechanisms independent of *vhnf1*.

Discussion

The involvement of extrinsic signals in otic induction has been extensively studied (Brigande et al., 2000; Fekete and Wu, 2002; Torres and Giraldez, 1998). In particular, Fgf signalling from the adjacent hindbrain has been shown to control early steps of otic induction (Maroon et al., 2002; Phillips et al., 2001; Represa et al., 1991). In contrast, the mechanisms underlying the patterning of the otic vesicle are still poorly understood. In this study, we have analysed in detail the patterning of the otic vesicle in the *vhnf1*^{hi2169} mutant line in order to further investigate the role of hindbrain signalling in this process. The *vhnf1* gene is expressed at late gastrula and early somite stages in the caudal hindbrain, up to a rostral limit that coincides with the prospective r4/r5 boundary. Within this domain, it is required for the activation of *val* expression in r5 and r6, and of *krx20* expression in r5 (Hernandez et al., 2004; Sun and Hopkins, 2001; Wiellette and Sive, 2003). While *vhnf1* is not expressed in the otic primordium, *vhnf1* mutants display rounded otic vesicles, suggesting a role for this gene upstream of hindbrain signals required for proper otic patterning. Our data indicate that the loss of *vhnf1* function leads to an anteriorisation of the entire otic vesicle. Interestingly, it also leads to a dorsal shift of cell groups, such as the future maculae, normally present within the ventral part of the vesicle. Finally, the size and distribution of the sensory and neurogenic epithelia are disturbed. Our results show that hindbrain signals are required for proper patterning of the zebrafish otic vesicle, not only along the AP axis, but also along the DV axis. Possible mechanisms linking hindbrain signalling to otic regionalisation are discussed below.

vhnf1 acts upstream of hindbrain signals required for AP patterning of the otic vesicle

It has been proposed that, in zebrafish, signals from the adjacent segmented hindbrain subdivide the otic vesicle along its AP axis. In this paper, we show that in *vhnf1* mutants, the anterior otic markers *nkx5.1*, *pax5* and *fgf8* are ectopically expressed in the caudal part of the otic vesicle. Conversely, the expression of the posterior marker *follistatin* is reduced. This expansion and/or duplication of anterior structures can be observed as early as the otic placode stage (14 hpf). Since this is the first stage when an asymmetry along the otic AP axis is detected, this result demonstrates that *vhnf1* is involved in the earliest steps of otic AP patterning.

The anteriorisation of the otic vesicle in *vhnf1* mutant embryos is reminiscent of the otic defects resulting from reduced Hh signalling in zebrafish embryos (Hammond et al., 2003). In both cases, the expression of the anterior marker *nkx5.1* is duplicated posteriorly and the expression of the posterior marker *follistatin* is hardly detectable. However, other anterior markers, such as *pax5* and *fgf8*, are not affected in *hh* mutants, suggesting that the anteriorisation of the otic vesicle is stronger in the *vhnf1* mutants. This similarity suggests that Hh and hindbrain signals might cooperate to specify the posterior otic identity.

The AP defects of *vhnf1* mutant ears are also similar to those observed in *val* mutants (Kwak et al., 2002). This is not surprising since *vhnf1* is required, together with Fgf signals from r4, to activate the expression of *val* in r5 and r6. However, the two phenotypes are distinct. In respect to patterning, only expansions – mainly medial – and no duplication of the anterior otic vesicle have been described for *val*. Other aspects of the phenotype are also different in these two mutants. For instance, the number, position and size of the sensory cristae are variable in *vhnf1* mutants, while in *val* mutants, the cristae develop normally (Kwak et al., 2002). Interestingly, DV patterning defects are present in both *val* (our unpublished data) and *vhnf1* (this paper) mutant ears, and they are much milder in *val* mutants. These different phenotypes suggest that *vhnf1* has functions in patterning the otic vesicle that are independent of *val*. This hypothesis is consistent with the observation made by Hernandez et al. (2004) that *vhnf1* regulates some aspects of rhombomere identity independently of *val*.

It has been proposed that the expansion of the anterior otic region in *val* mutants is due, at least in part, to an expansion of *fgf3* expression in the caudal hindbrain. Consistent with this hypothesis, depletion of *fgf3* and *fgf8* within the hindbrain after otic induction, leads to a loss of anterior structures of the otic vesicle (Haddon and Lewis, 1996; Leger and Brand, 2002; Maroon et al., 2002). This suggests that, in addition to being necessary for induction of the otic placode (Leger and Brand, 2002), Fgfs from the hindbrain are also involved in AP patterning of the zebrafish otic vesicle (Kwak et al., 2002; Leger and Brand, 2002). The stronger AP defects observed in *vhnf1* mutant ears compared to *val* mutants could be due to: i) an excess of Fgf signalling in the posterior hindbrain, and/or ii) a mechanism independent of Fgf signalling.

Altogether, our results demonstrate that in zebrafish, *vhnf1* is required to control signals from the segmented hindbrain involved in early AP patterning of the otic vesicle. We propose that *vhnf1* acts in part through the activation of *val* expression, and also in a *val* independent manner, possibly by synergizing with Hh signals from the ventral midline.

Hindbrain signalling is required for DV patterning of the otic vesicle in zebrafish

In addition to the AP patterning defects, *vhnf1* mutant embryos also display abnormalities in DV patterning of the otic vesicle. Several ventral cell groups are shifted dorsally while the dorsal part of the otic vesicle is severely reduced. This points to a new role of hindbrain signals in specifying cell position along the DV axis of the otic vesicle in zebrafish. This function of hindbrain signals in otic DV patterning is consistent with the data obtained in amniotes (Bok et al., 2005; Choo et al., 2006; Riccomagno et al., 2002, 2005). Although the structure and

function of the vestibular apparatus has been highly conserved in all vertebrates, the auditory chambers have undergone extensive evolutionary modification. The saccula, which is a prominent auditory organ in fish, serves a vestibular role in mammals and birds. The primary auditory organ in birds and mammals is the cochlea, which has no known counterpart in fishes and amphibians. In spite of these differences in the auditory structures, there is increasing evidence suggesting that the main mechanisms controlling otic patterning are quite similar among vertebrates (Riley and Phillips, 2003). The results obtained in the present study are in line with this hypothesis.

This raises the question of whether similar signals are involved in DV patterning of the otic vesicle in amniotes and in zebrafish. Wnt and Hh signals are involved in otic patterning in mice. On the one hand, Shh is necessary to specify ventral (auditory) cell fates within the mouse inner ear, both by directly controlling gene expression and by restricting the influence of Wnt signals (Riccomagno et al., 2002, 2005). As discussed previously, Hh signals have been involved in the specification of AP but not DV patterning of the zebrafish otic vesicle. On the other hand, Wnt1 and Wnt3a have been identified as the source of hindbrain signals required for the specification of the dorsal (vestibular) part of the otic vesicle (Riccomagno et al., 2005). Several *wnt* genes, including *wnt1* and *wnt3a* (Riley et al., 2004), are expressed in the dorsal neural tube in zebrafish. In this study we found that *wnt1* and *wnt3a* are downregulated in r5 and r6 *vhnf1* mutant embryos (Fig. 4). This suggests that Wnt signalling could link dorsal hindbrain to dorsal otic patterning in zebrafish and that the mechanisms involved in the specification of vestibular structures may be conserved among vertebrates.

Effects of vhnf1 inactivation on the organization of the sensory elements of the inner ear

Development of the first hair cells is normally restricted to regions of the otic placode directly adjacent to r4 and r6 (Haddon et al., 1998b) (Fig. 5), suggesting that signals emitted in these rhombomeres specify the equivalence groups from which hair cells emerge, or that signals from r5 repress their formation. Here we show that, in *vhnf1* mutants, the first hair cells form at ectopic positions all along the AP and DV axes of the otic vesicle. A similar phenotype has been reported in the *val* mutant ears and loss of *fgf3* function has been shown to rescue the excess of hair cells, suggesting that Fgf3 secreted from r4 is sufficient to specify hair cells in the otic vesicle (Kwak et al., 2002). We show here that the expansion of the presumptive sensory epithelium, marked by the expression of *delta* and *serrateB* lateral to r5 in *vhnf1* mutants, correlates with the reduction of r5 (Fig. 5). This result strongly suggests that an inhibitory signal from r5 normally restricts hair cell specification lateral to r4 and r6.

Parallel to the specification of the hair cells in the sensory patches, the neurons of the SAG are specified in the anteroventral part of the otic vesicle, the neurogenic epithelium. Neuroblasts delaminate from the ventral wall of the otocyst between 22 and 36 hpf, and differentiated neurons begin to be visible in the anteroventrally positioned ganglion by 24–30 hpf (Haddon and Lewis, 1996). In *vhnf1* homozygous mutants, the neurogenic domain is expanded. Since neuronal progenitors delaminate from the anteroventral region of the otic vesicle, we propose that this phenotype is a consequence of the anteriorisation and ventralisation of the *vhnf1* mutant inner ears. Moreover, *ngn1* and *neuroD*, which are normally expressed by the neuroblasts before they delaminate, remain expressed much after delamination has normally ended in a wild type ear, suggesting that the mechanisms responsible for the temporal control of neural specification are perturbed in *vhnf1* mutants. However, neither a duplication of this domain, nor an increase in the number of final neurons, nor a posterior expansion of the SAG were ever observed. One explanation would be that a survival factor is missing or is in a limited concentration and therefore ectopic neurons cannot proceed further. A similar observation has been made in the zebrafish Hh mutants, which also show a duplication of anterior otic markers (Hammond et al., 2003). However, it is interesting to note another difference with Hh mutant, that sensory organs are not mirror duplicated in *vhnf1* mutants, suggesting that though *vhnf1* may be involved in the earliest steps of AP patterning, it does not have such strong effect later as does Hh signalling.

Acknowledgments

The authors want to thank Dr. Nancy Hopkins for kindly providing the *vhnf1*^{hi2169} zebrafish mutant line, Marta Linares for excellent technical assistance, and Fernando Giraldez and Adam Cliffe for critical reading of the manuscript. The work was supported by grants from the Ministère de l'Education Nationale, de l'Enseignement Supérieure et de la Recherche and the Association pour la Recherche contre le Cancer to V.L., Ministerio de Educación y Ciencia BMC2003-07751-CO3-03 to C.P., Centre National de la Recherche Scientifique, Université Pierre et Marie Curie and Association pour la Recherche sur le Cancer to S.S.M., and "Programme International de Coopération Scientifique" (Generalitat de Catalunya-Centre National de la Recherche Scientifique) to C.P. and S.S.M.

References

Adamska, M., Leger, S., Brand, M., Hadrys, T., Braun, T., Bober, E., 2000. Inner ear and lateral line expression of a zebrafish Nkx5-1 gene and its downregulation in the ears of FGF8 mutant, ace. Mech. Dev. 97, 161–165.

Akimenko, M.A., Ekker, M., Wegner, J., Lin, W., Westerfield, M., 1994. Combinatorial expression of 3 zebrafish genes related to distal-less-part of A homeobox gene code for the head. J. Neurosci. 14, 3475–3486.

Andermann, P., Ungos, J., Raible, D.W., 2002. *Neurogenin1* defines zebrafish cranial sensory ganglia precursors. Dev. Biol. 251, 45–58.

Bauer, M.P., Goetz, F.W., 1998. Zebrafish mutagenesis: a screen for reproductive mutants. Biol. Reprod. 58, 104.

Blader, P., Rastegar, S., Fischer, N., Strahle, U., 1997. Cleavage of the BMP-4 antagonist chordin by zebrafish tolloid. Science 278, 1937–1940.

Bok, J., Bronner-Fraser, M., Wu, D.K., 2005. Role of the hindbrain in dorsoventral but not anteroposterior axial specification of the inner ear. Development 132, 2115–2124.

Brigande, J.V., Kiernan, A.E., Gao, X., Iten, L.E., Fekete, D.M., 2000. Molecular genetics of pattern formation in the inner ear: do compartment boundaries play a role? Proc. Natl. Acad. Sci. U. S. A. 97, 11700–11706.

Chang, W., Brigande, J.V., Fekete, D.M., Wu, D.K., 2004. The development of semicircular canals in the inner ear: role of FGFs in sensory cristae. Development 131, 4201–4211.

Choo, D., Ward, J., Reece, A., Dou, H., Lin, Z., Greinwald, J., 2006. Molecular mechanisms underlying inner ear patterning defects in *kreisler* mutants. Dev. Biol. 289, 308–317.

Ekker, M., Akimenko, M.A., Allende, M.L., Smith, R., Drouin, G., Langille, R.M., Weinberg, E.S., Westerfield, M., 1997. Relationships among *msx* gene structure and function in zebrafish and other vertebrates. Mol. Biol. Evol. 14, 1008–1022.

Fekete, D.M., 1999. Development of the vertebrate ear: insights from knockouts and mutants. Trends Neurosci. 22, 263–269.

Fekete, D.M., Wu, D.K., 2002. Revisiting cell fate specification in the inner ear. Curr. Opin. Neurobiol. 12, 35–42.

Giraldez, F., 1998. Regionalized organizing activity of the neural tube revealed by the regulation of lmx1 in the otic vesicle. Dev. Biol. 203, 189–200.

Haddon, C., Lewis, J., 1996. Early ear development in the embryo of the zebrafish, *Danio rerio*. J. Comp Neurol. 365, 113–128.

Haddon, C., Jiang, Y.J., Smithers, L., Lewis, J., 1998a. Delta-Notch signalling and the patterning of sensory cell differentiation in the zebrafish ear: evidence from the mind bomb mutant. Development 125, 4637–4644.

Haddon, C., Smithers, L., Schneider-Maunoury, S., Coche, T., Henrique, D., Lewis, J., 1998b. Multiple *delta* genes and lateral inhibition in zebrafish primary neurogenesis. Development 125, 359–370.

Hammond, K.L., Hill, R.E., Whitfield, T.T., Currie, P.D., 2002. Isolation of three zebrafish dachshund homologues and their expression in sensory organs, the central nervous system and pectoral fin buds. Mech. Dev. 112, 183–189.

Hammond, K.L., Loynes, H.E., Folarin, A.A., Smith, J., Whitfield, T.T., 2003. Hedgehog signalling is required for correct anteroposterior patterning of the zebrafish otic vesicle. Development 130, 1403–1417.

Hans, S., Liu, D., Westerfield, M., 2004. Pax8 and Pax2a function synergistically in otic specification, downstream of the Foxi1 and Dlx3b transcription factors. Development 131, 5091–5102.

Hauptmann, G., Gerster, T., 1994. 2-Color whole-mount in-situ hybridization to vertebrate and Drosophila embryos. Trends Genet. 10, 266.

Hernandez, R.E., Rikhof, H.A., Bachmann, R., Moens, C.B., 2004. *vhnf1* integrates global RA patterning and local FGF signals to direct posterior hindbrain development in zebrafish. Development 131, 4511–4520.

Itoh, M., Chitnis, A.B., 2001. Expression of proneural and neurogenic genes in the zebrafish lateral line primordium correlates with selection of hair cell fate in neuromasts. Mech. Dev. 102, 263–266.

Kimmel, C.B., Ballard, W.W., Kimmel, S.R., Ullmann, B., Schilling, T.F., 1995. Stages of embryonic-development of the zebrafish. Dev. Dyn. 203, 253–310.

Krauss, S., Johansen, T., Korzh, V., Moens, U., Ericson, J.U., Fjose, A., 1991. Zebrafish *pax2a*–a paired box–containing gene expressed in the neural-tube. EMBO J. 10, 3609–3619.

Krauss, S., Korzh, V., Fjose, A., Johansen, T., 1992. Expression of four zebrafish wnt-related genes during embryogenesis. Development 116, 249–259.

Kwak, S.J., Phillips, B.T., Heck, R., Riley, B.B., 2002. An expanded domain of *fgf3* expression in the hindbrain of zebrafish *valentino* mutants results in mis-patterning of the otic vesicle. Development 129, 5279–5287.

Lecaudey, V., Anselme, I., Rosa, F., Schneider-Maunoury, S., 2004. The zebrafish Iroquois gene *iro7* positions the r4/r5 boundary and controls neurogenesis in the rostral hindbrain. Development 131, 3121–3131.

Leger, S., Brand, M., 2002. *Fgf8* and *Fgf3* are required for zebrafish ear placode induction, maintenance and inner ear patterning. Mech. Dev. 119, 91–108.

Maroon, H., Walshe, J., Mahmood, R., Kiefer, P., Dickson, C., Mason, I., 2002. *Fgf3* and *Fgf8* are required together for formation of the otic placode and vesicle. Development 129, 2099–2108.

Maves, L., Jackman, W., Kimmel, C.B., 2002. FGF3 and FGF8 mediate a rhombomere 4 signaling activity in the zebrafish hindbrain. Development 129, 3825–3837.

Molven, A., Njolstad, P.R., Fjose, A., 1991. Genomic structure and restricted neural expression of the zebrafish wnt-1 (int-1) gene. EMBO J. 10, 799–807.

Mowbray, C., Hammerschmidt, M., Whitfield, T.T., 2001. Expression of BMP signalling pathway members in the developing zebrafish inner ear and lateral line. Mech. Dev. 108, 179–184.

Oxtoby, E., Jowett, T., 1993. Cloning of the zebrafish Krox-20 Gene (Krx-20) and its expression during hindbrain development. Nucleic Acids Res. 21, 1087–1095.

Pfeffer, P.L., Gerster, T., Lun, K., Brand, M., Busslinger, M., 1998. Characterization of three novel members of the zebrafish Pax2/5/8 family: dependency of *Pax5* and *Pax8* expression on the *Pax2.1* (noi) function. Development 125, 3063–3074.

Phillips, B.T., Bolding, K., Riley, B.B., 2001. Zebrafish *fgf3* and *fgf8* encode redundant functions required for otic placode induction. Dev. Biol. 235, 351–365.

Reifers, F., Bohli, H., Walsh, E.C., Crossley, P.H., Stainier, D.Y., Brand, M., 1998. Fgf8 is mutated in zebrafish acerebellar (*ace*) mutants and is required for maintenance of midbrain–hindbrain boundary development and somitogenesis. Development 125, 2381–2395.

Represa, J., Leon, Y., Miner, C., Giraldez, F., 1991. The *int-2* proto-oncogene is responsible for induction of the inner ear. Nature 353, 561–563.

Riccomagno, M.M., Martinu, L., Mulheisen, M., Wu, D.K., Epstein, D.J., 2002. Specification of the mammalian cochlea is dependent on Sonic hedgehog. Genes Dev. 16, 2365–2378.

Riccomagno, M.M., Takada, S., Epstein, D.J., 2005. Wnt-dependent regulation of inner ear morphogenesis is balanced by the opposing and supporting roles of Shh. Genes Dev. 19, 1612–1623.

Riley, B.B., Phillips, B.T., 2003. Ringing in the new ear: resolution of cell interactions in otic development. Dev. Biol. 261, 289–312.

Riley, B.B., Zhu, C., Janetopoulos, C., Aufderheide, K.J., 1997. A critical period of ear development controlled by distinct populations of ciliated cells in the zebrafish. Dev. Biol. 191, 191–201.

Riley, B.B., Chiang, M.Y., Storch, E.M., Heck, R., Buckles, G.R., Lekven, A.C., 2004. Rhombomere boundaries are Wnt signaling centers that regulate metameric patterning in the zebrafish hindbrain. Dev. Dyn. 231, 278–291.

Sahly, I., Andermann, P., Petit, C., 1999. The zebrafish *eya1* gene and its expression pattern during embryogenesis. Dev. Genes Evol. 209, 399–410.

Sun, Z., Hopkins, N., 2001. *vhnf1*, the MODY5 and familial GCKD-associated gene, regulates regional specification of the zebrafish gut, pronephros, and hindbrain. Genes Dev. 15, 3217–3229.

Sun, Z., Shi, K., Su, Y., Meng, A., 2002. A novel zinc finger transcription factor resembles *krox-20* in structure and in expression pattern in zebrafish. Mech. Dev. 114, 133–135.

Torres, M., Giraldez, F., 1998. The development of the vertebrate inner ear. Mech. Dev. 71, 5–21.

Walshe, J., Maroon, H., McGonnell, I.M., Dickson, C., Mason, I., 2002. Establishment of hindbrain segmental identity requires signaling by FGF3 and FGF8. Curr. Biol. 12, 1117–1123.

Westerfield, M., 1995. The Zebrafish Book. University of Oregon Press.

Whitfield, T.T., Riley, B.B., Chiang, M.Y., Phillips, B., 2002. Development of the zebrafish inner ear. Dev. Dyn. 223, 427–458.

Wiellette, E.L., Sive, H., 2003. *vhnf1* and *Fgf* signals synergize to specify rhombomere identity in the zebrafish hindbrain. Development 130, 3821–3829.